

ARTICLE

Corrosion of nm-sized Gold by A Novel Two-dimensional Atomic Structure with Copper

Received 00th January 20xx,
Accepted 00th January 20xx

Hidetaka Sawada, ^{*a,b,c} Konstantin B. Borisenko ^b, Eiji Okunishi ^{a,b}, and Angus I. Kirkland ^{a,b}

DOI: 10.1039/x0xx00000x

A nm-sized gold can be corroded in air in the presence of copper at room temperature during ageing to form a compound of gold. The compound is a belt-like two-dimensional material. The structure consists of a linear arrangement of atomic columns with an interval of 0.5 nm and with the structure extending perpendicular to these rows. Using high-resolution electron microscopy and chemical analyses, the structure within each row of atomic columns is determined to be a hexagonal arrangement of gold, with copper. An atomic model of this two-dimensional structure consisting of gold, copper, and oxygen is constructed and optimized using DFT calculations. This study has direct relevance to the use of gold as a contact material in semiconductor devices.

Introduction

In high-technology engineering of semiconducting devices, Au is frequently used for fine wire bonding due to its high electrical conductivity^{1,2} and chemical inertness which allows constant conductivity during electrical operation over long periods of time^{3,4}. However, as integrated circuits become denser and electrical devices become smaller according to Moore's law it is essential that nm-sized Au shows chemical and structural stability under normal operating temperatures and atmospheric conditions, to avoid potential degradation of device performance. In this study, we show that nm-sized Au can be corroded in air in the presence of Cu at room temperature during ageing to form a compound of Au. The compound consists of a belt-like two-dimensional material containing Au, Cu and O.

Two-dimensional layered materials such as graphene, hexagonal boron nitride, and metal dichalcogenides have been shown to have a range of technologically important applications^{5,6}. Combining these materials has the potential to further develop materials that have new properties within low dimensional structures. For this reason, the discovery of new two-dimensional materials is expected to expand the variety of possible applications and devices. It has been suggested⁵ that only a limited range of possible atomic species can have stable two-dimensional structures and metals such as Cu, Au, and Ag are not considered as suitable candidates. Although a wide variety of Au nanostructures have been reported, including,

nanoparticles⁷, nanorods⁸, nanosheets⁹, and nanowires¹⁰, there have been no reports of a stable two-dimensional material containing Au. Here, we report the first observation of a two-dimensional material containing Au that has been using transmission electron microscopy/scanning transmission electron microscopy (TEM/STEM).

Experimental

Cu was initially vacuum evaporated using a W filament in the absence of any sample leaving a small amount of residual Cu on the W wire (Figs.1(a,b)). A few mg of Au were then deposited onto a TEM grid coated with a C film (Fig. 1(d)) using the same filament (Fig.1(c)). During deposition of Au, the residual Cu was also evaporated. After deposition, Au nanoparticles were deposited on a TEM grid coated with a carbon film. The residual Cu on the W wire was co-deposited, although Cu was not clearly visible in the deposited film immediately after deposition in TEM (Fig. 1(e)).

<Figure 1>

^a Department of Materials, University of Oxford, Parks Road, Oxford OX1 3PH, UK

^b Electron Physical Sciences Imaging Centre (ePSIC), Diamond Light Source Ltd, Didcot, Oxford, OX11 0DE, UK

^c JEOL Ltd, 3-1-2 Musashino, Akishima, Tokyo, 196-8558, Japan.

Electronic Supplementary Information (ESI) available: [details of any supplementary information available should be included here]. See DOI: 10.1039/x0xx00000x

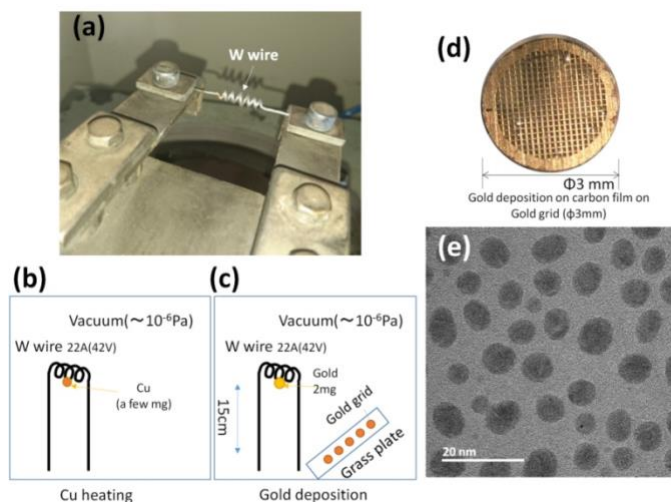


Fig 1. (a) W wire in vacuum a chamber used for deposition, (b) schematic of the W filament with Cu, (c) schematic of the W filament with Au and grids, (d) Au TEM grid with a C film (AGS160AH, Agar Scientific), (e) TEM image of deposited Au particles. A few mg of Cu wire was initially attached to a W filament (Fig. 1(a) and 1(b)). The Cu was heated with a current of 22 A at a voltage of 42 V and evaporated without a specimen grid in the deposition chamber. This left residual Cu on the W wire. Au wire with a weight of approximately 2 mg was then attached to the W wire (Fig. 1(c)) for deposition onto TEM grids (Fig. 1(d)) under vacuum using the same W filament with a current of 22 A and a voltage of 42 V.

Results

Observation of the particles after seven days exposure to air showed that small amounts of non-crystalline Cu, as indicated by orange arrows in Fig. 2(a), was attached to the Au particles. The film was then stored in air at RT for approximately one hundred days for further ageing. The aged film showed belt-like structures with a large lattice spacing, as indicated by yellow arrows, in Fig. 2(b) around the Au particles, suggesting that a slow oxidation process is responsible for their growth.

<Figure 2>

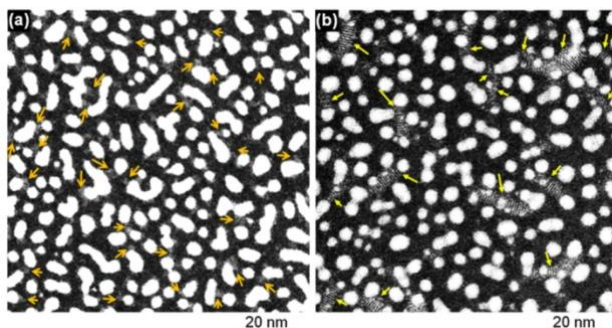


Fig. 2. (a) STEM dark field image of deposited film after one week, showing Au particles with regions of non-crystalline Cu (orange arrows). (b) STEM dark field image of deposited film after one hundred days aging showing Au particles and belt-like two-dimensional structures (yellow arrows). Although the amorphous carbon film

cannot be seen in STEM dark field image, it is clearly seen in STEM bright field (BF) (Supplemental Information 1).

Figure 3(a) shows a high-resolution STEM dark field (DF) image of the aged film, with 5–15 nm Au particles visible in bright (white) contrast. Around the particles, there are belt-like structures indicated by yellow arrows. These have shorter widths (approximately 2–5 nm) and longer lengths (approximately 5–20 nm). We denote these structures as “pedestrian crossing structures” (PCS). We have also observed much larger PCS, as shown in Supplemental Information 3. The distance between the basal planes in the PCS (perpendicular to the direction of elongation) was determined to be 0.5 ± 0.01 nm from images (Fig. 3(b)). The intensity in the dark field image of the PCS is lower than that of the Au particles with similar projected diameters, indicating that the PCS are thin structures along the beam direction. The measured thickness of the PCS was determined to be 2–5 atomic layers (Supplemental Information 2).

<Figure 3>

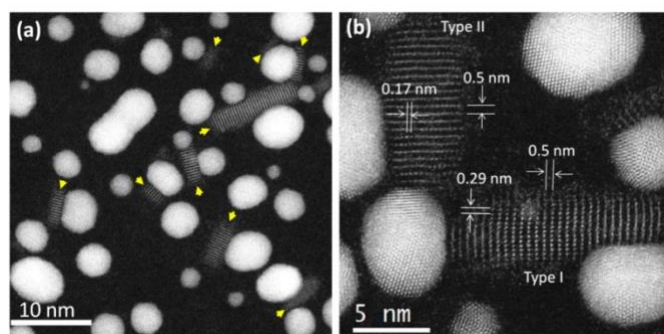


Fig. 3. (a) Dark field STEM image of Au particles with PCS indicated by yellow arrows, recorded at 300 kV. (b) High-resolution dark field STEM image of the PCS. The PCS structure has periodic rows of atomic columns with a distance perpendicular to the long axis of 0.5 nm. Two types of PCS with differing atomic distances perpendicular to the basal plane were observed: type I has a periodicity of 0.29 ± 0.01 nm, and type II has a periodicity of 0.17 ± 0.01 nm, as shown in Fig. 3(b).

Figure 4 shows an electron energy loss spectrum (EELS) recorded in STEM mode. Figure 4(a) shows the region used to acquire a line spectrum from the C film, PCS, and a Au particle, indicated by the green line. The EELS M edge of the gold obtained from a Au particle, is shown in Fig. 4(b). The Au M signal was also detected in the region of the PCS, as shown in Fig. 4(c). Figure 4(d) shows superimposed traces of the STEM dark field image intensity (blue line) and the intensity of the EELS signal after background subtraction (light green). The higher intensity parts of the line profile in the dark field STEM images have a higher Au signal in the EELS, indicating that high contrast features in the PCS contain Au atoms; EELS revealed

that the rows of atomic columns in the PCS consist primarily of Au.

<Figure 4>

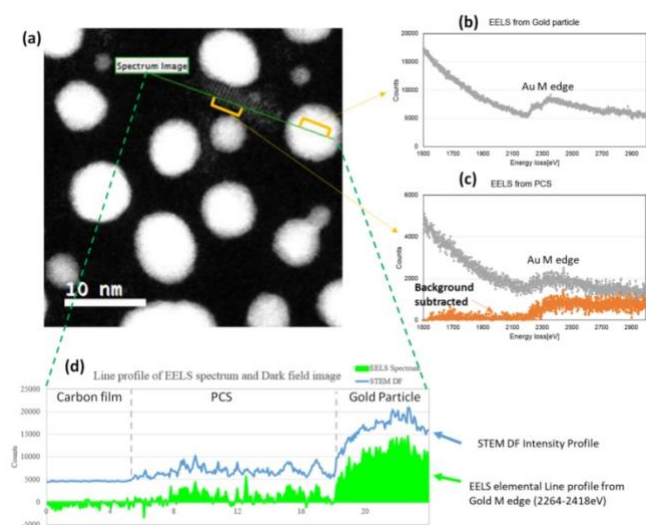


Fig. 4. (a) Survey image for EELS spectrum imaging recorded at an accelerating voltage of 200 kV using a Gatan Quantum ER fitted to a JEM-ARM200F equipped with a cold field emission gun. Line spectrum of 300 points were taken with an acquisition time for each pixel of 0.1s. The beam current was 200 pA with a convergence semi angle of 23 mrad. The spectrum line profile was taken from the C film, PCS and a Au particle, as indicated by the green line. (b) Spectrum from Au particles indicated in the region marked in orange in (a). (c) Spectrum intensity and background subtracted spectrum from the PCS. (d) Background subtracted Au M edge signal (2264–2418 eV) and intensity profile of the STEM dark field image from the PCS.

Figure 5(a) shows a STEM image of the carbon film with Au deposition after ageing. The power spectrum calculated from Fig. 5(a) is shown in Fig. 5(b) with spots from the basal line of PCS indicated by yellow circles, correspond to spacings of $(0.50 \text{ nm})^{-1}$. PCS were observed around the Au particles, as shown in Fig. 5(b). Typically, the PCS structures were extended tangentially to the Au particles. Au particles attached to the PCS are truncated on the side where the PCS is attached, whereas Au particles without PCS are round (Fig. 5(a)). This indicates that the Au particle is the likely source of atoms used to synthesize the PCS; A nm-sized gold can be corroded in air at room temperature during ageing to form a compound of gold.

<Figure 5>

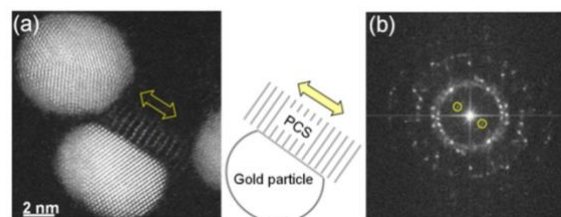


Fig. 5. (a) PCS attached to a Au particle with a schematic diagram. (b) Power spectrum calculated from the image in (a). The spots highlighted correspond to spacing of $(0.50 \text{ nm})^{-1}$ (Supplemental Information 5).

Figure 6(a) shows an under-focused TEM image of a PCS in which the dark contrast corresponds to atomic column positions. As indicated by the yellow arrows in Fig. 6(a), the strong contrast correspond to Au atomic columns with a weak contrast observed between these positions, as indicated by the light green arrow. Figure 6(b) shows an over-defocused image of a PCS. In this case, white contrast corresponds to the position of the atomic columns, and strong white contrast (indicated by yellow arrows) show the Au atomic columns, as well. Weak white contrast indicated by the light green arrow is visible between the Au columns. These results indicate that there is a lighter atom situated between the Au lines, which have a spacing of 0.5 nm.

<Figure 6>

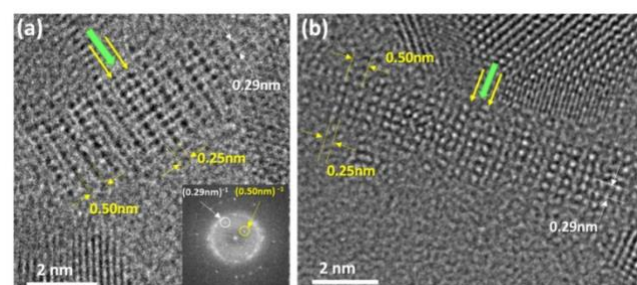


Fig. 6. (a) Under-defocused TEM image of a PCS recorded at 200 kV ($C_s = -1 \mu\text{m}$, and defocus = -12 nm). The power spectrum is displayed lower right. (b) Over-defocused TEM image of PCS at 300 kV ($C_s = -1 \mu\text{m}$, and defocus = 10 nm).

TEM image contrast indicates that there are lighter atoms between the Au atomic columns. Figure 7(a) shows a STEM dark field image of PCS, and figures 7 (b-d) shows energy dispersive spectroscopy (EDS) spectrum mappings from a PCS with several gold particles. EDS analysis with two JED 158 mm² SDDs detectors was performed with a current of 35 pA using a convergent semi-angle of 24 mrad at 80 kV with the solid angle of 2.21 sr. Mapping in Fig. 7(b) shows strong white contrast in Fig. 7(a) and 7(g) is gold particles. The position of gold particles is indicated by yellow circles and PCS is indicated by a white line in Figs. 7 (f-j). Figure 7(c) and 7(h) shows Cu X-ray single

detected from PCS and gold particles, indicating Cu was contained in gold particles and PCS. Cu signal was detected in the EDS spectrum from the region of PCS in Fig.7 (k). Cu in PCS has been identified using EELS, as well (Supplemental Information 4). Although O signal was detected in the EDS spectrum from the region of PCS in Fig.7 (k), there exists O uniformly in a carbon film as shown in Fig.7(d) and 7(i).

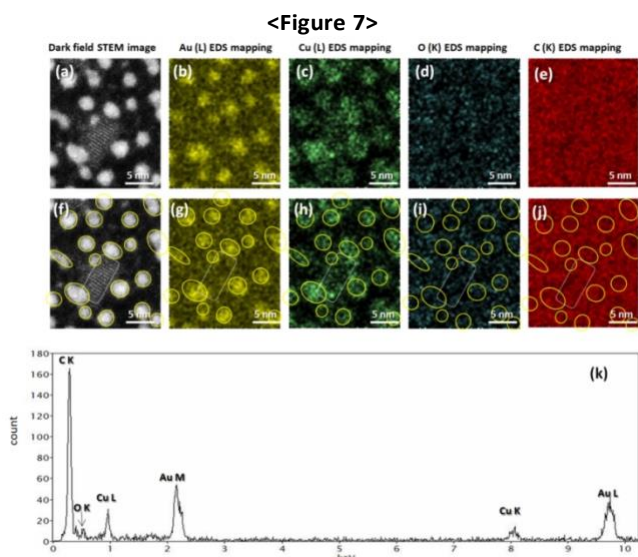


Fig. 7. (a,f) STEM dark field image of a PCS and EDS mapping data of (b,g) Au, (c,h) Cu, and (d,i) O from the area of 90 pixel and 105 pixel (0.195 nm/pixel) with 94 times summation with acquisition time of 0.5 ms/pixel at 80kV using JEM-ARM300F. (k) The spectrum is taken from area of PCS. The specimen was made on the carbon film on gold grid. C was detected from the carbon film.

Discussion

From our experimental observations, we propose that the structure of the PCS consists of Cu-O layers sandwiched between Au layers. Using this hypothesis, an atomic model of the PCS was constructed and optimized using the density functional theory (DFT) calculations including energy optimizations and band structure calculations were performed using the CASTEP software¹¹. Full details of the calculations are described in Supplemental Information 6. It indicates that this 2D materials is a semiconductor with a narrow band gap, < 0.1 eV from the band structure. If PCS would grow around Au fine wire bonding in nano devices, it may cause failure in the electric contact. The structure optimized using DFT is shown in Fig. 8(a), 8(b), and 8(c). The distance between the Au planes in the relaxed structure is 0.44 nm, similar to our experimental observations (Fig. 8). Figure 8(d) shows a TEM image recorded at an accelerating voltage of 300 kV. The atomic positions are observed in negative contrast and the higher contrast position corresponds to the Au atomic columns. An image simulated using the calculated structure is shown inset.

<Figure 8>

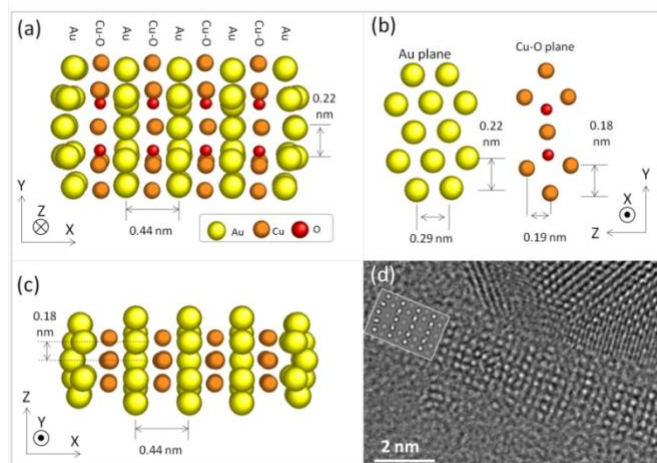


Fig. 8. (a) The proposed PCS structure in the X-Y projection, (b) Y-Z projection of the atomic structure showing the Au and Cu-O planes, (c) X-Z projection of the atomic structure of PCS. (d) Aberration-corrected TEM image (Overfocus = 4 nm, Cc= 1.6 nm, V= 300kV, and ΔE = 0.45 eV) of the PCS with an image simulation based on the DFT optimized structure in (a) inset.

Gold nanoparticles have been investigated as a possible additive in organic solar cells due to their plasmonic properties¹². In general, material for solar cell nanoparticles has a narrow band-gap to increase absorption of light. For example, CdS, PbS nanoparticles are used. PCS offers a unique combination of plasmonic gold nanoparticle with a narrow band-gap semiconductor PCS which are non-toxic (compared to Cd and Pb) and have a potential to increase efficiency of solar cells.

Conclusions

This study has shown an elongated 2D structure consisting of Au, Cu and O formed after extended air exposure of metallic nano gold with trace amounts of copper. The structure has a periodicity of 0.5 nm along the elongation direction and consists of alternating Au and Cu-O planes. The thickness of the structure is between 2 and 5 atomic layers. An atomic model containing Au, Cu and O atoms is proposed and optimized using DFT. The fact that a nm-sized gold can be corroded in air in the presence of copper at room temperature has direct relevance to the use of gold as a contact material.

Conflicts of interest

There are no conflicts to declare.

Acknowledgements

H.S and A.K thank Shanshan Wang and Jamie H. Warner for discussions about specimen preparation and G. Cook and C.

Salter for assisting with specimen preparation. H.S also thanks Y. Moriya, K. Yajima, A. Yamagishi, and Yu-Jen Chou for discussions about specimen preparation, F. Hosokawa for the image simulation software, M. Danaie and C. S. Allen for the specimen treatment, and I. Ohnishi, H. Hashiguchi, and L. Jones for the EDS analysis. K.B would like to acknowledge the use of the University of Oxford Advanced Research Computing (ARC) facility in carrying out this work. <http://dx.doi.org/10.5281/zenodo.22558>.

References

- 1 S. Tomiyama and Y. Fukui, Gold Bulletin, 1995, **15**, 43-50.
- 2 G.Qi, and S. Zhang, Journal of Materials Processing Technology, 1998, **68**, 288-293.
- 3 B. Hammer and J. K. Norskov, Nature, 1995, **376**, 238–240.
- 4 T. W. Ellis, Gold Bulletin, 2004, **37**, 66-71.
- 5 A. K. Geim and I. V. Grigorieva, Nature, 2013, **499**, 419-42 .
- 6 M. Chhowalla, H. S. Shin, G. Eda, L-J. Li, K. P. Loh and H. Zhang, Nature Chemistry, 2013, **5**, 263-275.
- 7 T. Takei, T. Akita, I. Nakamura, T. Fujitani, M. Okumura, K. Okazaki, J. Huang, T. Ishida and M. Haruta, Advances in Catalysis, 2012, **55**, 1-124.
- 8 J. Pérez-Juste, I. Pastoriza-Santos, L. Liz-Marzán, and P. Mulvaney, Coordination Chemistry Reviews, 2005, **249**, 1870-1901.
- 9 Q. Chen, K. He, A. Robertson, A. Kirkland and J. Warner, ACS Nano, 2016, **10**, 10418-10427 .
- 10 Y. Kondo, and K. Takayanagi, Science, 2000, **289**, 606-608.
- 11 S. J. Clark, M. D. Segall, C. J. Pickard, P. J. Hasnip, M. J. Probert, K. Refson and C. Payne, Z. Kristallogr, 2005, **220**, 567-570.
- 12 T. Kim, H. Kang, S. Jeong, D. J. Kang, C. Lee, C. Lee, M. Seo, J. Lee and B. J. Kim, ACS Applied Materials and Interfaces. 2014, **6**, 16956-16965.